Journal of Molecular Structure 1035 (2013) 69–75

Contents lists available at SciVerse ScienceDirect

Journal of Molecular Structure

journal homepage: www.elsevier.com/locate/molstruc

Combined theoretical and experimental study on the molecular structure, FT-IR, and NMR spectra of cyadox and 1,4-bisdesoxycyadox

Zongyang Li, Jiaheng Zhang, Yubo Li, Haixiang Gao *

Department of Applied Chemistry, China Agricultural University, Yuanmingyuan West Road 2#, Haidian District, Beijing 100194, China

HIGHLIGHTS

- 1,4-Bisdesoxycyadox (1,4-BDC) were synthesised as one of cyadox's main metabolite.
- Theoretically optimized structure agree very well with the experimental findings of BDOC.
- BDOC was characterized by IR, 1H, 13C NMR spectra.
- Bond dissociation enthalpies of N—O in BDOC were estimated theoretically.

ARTICLE INFO

Article history:
Received 18 July 2012
Received in revised form 29 August 2012
Accepted 12 September 2012
Available online 21 September 2012

Keywords:
Cyadox
1,4-Bisdesoxymequindox
Metabolite
Infrared spectra
NMR
BDE

ABSTRACT

1,4-Bisdesoxycyadox, a deoxidized metabolite of cyadox, was synthesised and characterized. Structural and conformational analyses were performed using theoretical calculations employing density functional theory (DFT). The molecular geometry was optimized using B3LYP method with 6-311+G(d,p) basis set and then it was compared with X-ray diffraction data of similar molecular compounds. From the optimized geometry of the molecule, vibrational frequencies of the title compounds were calculated via B3LYP/6-311+G(d,p) approach. The ^{1}H and ^{13}C NMR chemical shift were calculated by gauge-including atomic orbital method with B3LYP/6-311++G(2df,2pd) approach. Comparison of the experimental and calculated 1H and 13C chemical shifts resulted in the reliable assignment of cyadox and 1,4-bisdesoxycyadox. The first, second, total, and mean N—O bond dissociation enthalpies were also obtained theoretically.

1. Introduction

Quinoxaline-1,4-dioxide (QdNO) derivatives, which are benzoheterocycles composed of a quinoxaline ring and one or two acyclic chains, share the 1,4-di-N-oxide moiety and the accessory biological properties [1]. Due to their specific antibacterial activity against gram-negative bacteria, such as *Escherichia coli, Salmonella,* and *Pasteurella*, some QdNOs are widely utilized in the pharmaceutical and veterinary fields [2]. Cyadox, (2-quinoxalinyl-methylee)hydrazine N,N′-dioxide, is one of the notable QdNOs structurally related to carbadox, olaquindox, mequindox, and quinocetone. As a synthetic growth promoter, cyadox provides better growth-enhancing functions in food-producing animals, such as pigs, fish, goats, and poultry. However, problems pertaining to the toxicity of cyadox limit its application [3].

Based on previous in vitro studies of QdNO derivatives, some correlations exist between the degree of toxicity and the formation of QdNO drugs' metabolites [4]. Moreover, certain metabolites of quinoxaline-1,4-dioxide derivatives, especially their desoxy compounds, are suspected carcinogens and mutagens that cause severe side effects, thus triggering safety concerns [5]. The cleavage of N—O bond in QdNO drugs draws extensive attention because of its toxicological and pharmacological significance. According to Huang et al.'s research, cyadox is mainly metabolized to its deoxidized metabolites in the microsomes [6]. Therefore, studies on the mechanism of N-oxide reduction and detailed structure-related parameters of desoxy metabolites are imperative for the evaluation of cyadox risk. Currently, the most extensively studied metabolism profile of cyadox is represented via ultrahigh-performance liquid chromatography/electrospray ionization quadruple time-of-flight mass spectrometry (UPLC/ESI-QTOF-MS) combined with an algorithm software [7]. Alternatively, the direct measurement of the peak area ratio of the standard metabolite synthesis to the internal standards in an HPLC system is a more practical method of obtaining useful and direct pharmacokinetic information.

In this study, 1,4-bisdesoxycyadox (1,4-BDC) is synthesised as the main metabolite of cyadox. A comparison of the theoretical

* Corresponding author. Tel.: +86 1062731991; fax: +86 1062733830.
E-mail address: hxgao@cau.edu.cn (H. Gao).

0022-2860/$ - see front matter © 2012 Elsevier B.V. All rights reserved.
http://dx.doi.org/10.1016/j.molstruc.2012.09.030

and experimental infrared (IR) and nuclear magnetic resonance (NMR) spectra for the title compounds is reported. This study aims to determine the use of density functional theory (DFT) in predicting and evaluating spectroscopic properties and to elucidate the structural differences between cyadox and 1,4-bisdesoxycyadox. In addition, the N—O bond strength of cyadox measured by the N—O bond dissociation enthalpies (BDEs) is initially investigated by DFT calculation.

2. Experimental

2.1. Materials and measurements

Cyadox (98% purity) was provided by the College of Veterinary Medicine, Huazhong Agricultural University (Wuhan, China). Other reagents and solvents used in the synthesis were of analytical grade and purchased from Beijing Chemical Reagent Company. Melting points were measured with a WRX-4 micro melting point apparatus (Shanghai Yice Co., China). The infrared spectrum was recorded on a PerkinElmer FT-IR Spectrum 100 spectrometer in the spectral range 450 cm^{-1} to 4000 cm^{-1} with a scanning speed of 10 cm^{-1} min^{-1} and a resolution of 4.0 cm^{-1}. NMR was recorded for diluted solutions in DMSO using a BrukerDSX-300 at 300 MHz for ^{1}H and 75 MHz for ^{13}C. The chemical shifts were expressed in ppm relative to TMS.

2.2. Calculations

The molecular structures of the compounds in the ground state (in vacuo) were optimized using DFT method B3LYP level of theory, which combines Becke's three parameter non-local exchange functional with Lee–Yang–Parr's correlation functional together with the 6-311+G(d,p) basis set [8–10]. Frequency calculations at the 6-311+G(d,p) level were performed to identify all of the stationary points as minima and to provide free energies at 298.15 K, which include entropic contributions by considering the vibrational, rotational, and translational motions of the species. The calculated chemical shifts of ^{1}H NMR and ^{13}C NMR for the title compounds were obtained by gauge-including atomic orbital (GIAO) method using the B3LYP/6-311++G(2df,2dp) level of theory. NMR calculations were performed using the optimized geometries at the same level of theory with TMS as reference. The effect of DMSO solvent on the theoretical NMR parameters was evaluated using the default integral-equation-formalism polarizable continuum model (IEF–PCM) [11]. The N—O BDE is the calculated enthalpy change from the hemolytic bond dissociation reaction:

$$R—N—O\ (g) \rightarrow R—N^{\cdot}\ (g) + O^{\cdot}\ (g) \quad (1)$$

The mean N—O bond dissociation enthalpy of quinocetone is half of the enthalpy of the following reaction:

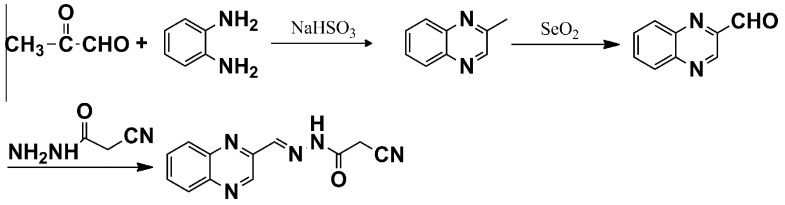

Fig. 1. Synthetic outline of the 1,4-bisdesoxymequindox.

Table 1
Geometrical data of cyadox and 1,4-BDC.

Bond length (Å)	Cyadox	1,4-BDC	Exp.	Bond angle (°)	Cyadox	1,4-BDC	Exp.
C1—N12	1.359	1.32	1.357	C2—N12—C1	118.2	117.9	121.3
C1—28C	1.398	1.426	1.406	N12—C1—C28	120.4	120.7	117.5
C2—N12	1.399	1.352	1.388	C1—C28—N13	123.2	122.7	125.2
C2—C3	1.407	1.427	1.401	C28—N13—C3	117.5	117.4	116.8
C2—C5	1.401	1.415	1.404	N13—C3—C2	120.1	120.4	121.6
C3—C6	1.399	1.412	1.401	C8—C5—C2	119.3	119.8	120.6
C3—N13	1.403	1.357	1.38	C5—C2—C3	119.9	119.4	120.9
N13—C28	1.341	1.308	1.309	C2—C3—C6	120.2	119.5	119
N12—O14	1.273		1.296	C3—C6—C7	119.3	119.7	119.9
N13—O15	1.270			C7—C8—C5	120.7	120.8	121.5
C5—C8	1.375	1.369	1.359	O14—N12—C1	121.6		
C8—C7	1.406	1.415	1.405	O15—N13—C28	122.0		
C7—C6	1.375	1.37	1.377	C1—C16—N18	129.3	131.1	
C1—C16	1.467	1.477		C15—N18—N19	121.3	121.6	
C16—N18	1.281	1.281		N18—N19—C21	121.6	121.6	
N18—N19	1.351	1.353		N19—C21—O27	120.4	120.5	
N19—C21	1.384	1.381		O27—C21—C22	124.7	124.5	
C21—O27	1.206	1.207		C21—C22—C25	112.6	112.6	
C21—C22	1.527	1.528		C22—C25—N26	177.4	177.3	
C22—C25	1.455	1.455		Selected dihedral angles (°)			
C25—N26	1.148	1.48		C2—N12—C1—C16	−174.8	−175.3	
C5—H4	1.079	1.081	0.95	C1—C15—N18—N19	5.1	5.3	
C8—H11	1.081	1.081	0.95	C18—C19—C21—C22	6.4	6.5	
C7—H10	1.081	1.081	0.95	C19—C21—C22—C25	178.6	179	
C6—H9	1.079	1.081	0.95	C21—C22—C25—N26	−179.2	−179.2	
C28—H29	1.077	1.084					
C16—H17	1.082	1.084					
N19—H20	1.015	1.014					
C22—H23	1.091	1.091					
C22—H24	1.091	1.091					

$$O{-}N{-}R{-}N{-}O\ (g) \rightarrow {\cdot}N{-}R{-}N{\cdot}\ (g) + 2O{\cdot}\ (g) \quad (2)$$

The bond dissociation energy of the N—O bond is computed from the heat formation at 298.15 K of the species involved in the dissociation, i.e.,

$$E_{BDE} = \Delta_f H^{\circ}_{298.15,R-N} + \Delta_f H^{\circ}_{298.15,O} - \Delta_f H^{\circ}_{298.15,R-N-O} \quad (3)$$

All theoretical properties were calculated using the Gaussian 09 program [12]. The obtained theoretical results aided in making detailed assignments of the experimental IR and NMR spectra.

2.3. Synthesis

2.3.1. Synthesis of 2-methylquinoxaline

Sodiumhydrogensulfite (24.5 g) was added to a 40% methylglyoxal (21.3 g) solution mixed with 50 ml water and then stirred. O-phenylenediamine (10.8 g) was dissolved in water (55 ml) with heating and transferred to a 500 ml round-bottom flask. After stirring for 20 min, the solvent was placed in the dark and stored overnight. After the addition of sodium metabisulfite (20 g) the mixture was extracted with 120 mL (3 × 40 mL) ether. Then the combined organic phase was washed with 30 mL water (3 × 10 mL). The solution was dried over anhydrous $MgSO_4$ and concentrated under reduced pressure. Oily liquid was obtained, with a yield of 11 g (51%). ^{1}H-NMR ($CDCl_3$):δ = 2.75 (CH_3, 3H, s), 7.70 (Ph—H, 2H, m), 8.02 (Ph—H, 2H, m), 8.72(N=CH, 1H, s); ^{13}C-NMR($CDCl_3$):δ = 22.3, 128.4, 128.6, 128.9, 129.8, 140.7, 141.837, 145.7, 143.5 ppm. Bp = 245.2–246.9 °C.

2.3.2. Synthesis of quinoxaline-2-carbaldehyde

2-Methyl-quinoxaline (11 g) in a 250 ml round-bottom flask was dissolved with dioxane and heated at 70 °C. A mixture of selenium dioxide (8.5 g) with dioxane (29 ml) and water (5.9 ml) was added dropwise into the flask within 90 min. The solution was then stirred at 85 °C for 4 h, and then filtered and processed with activated carbon for 30 min. Dioxane was distilled under reduced pressure and the residue was extracted with 30 mL (3 × 10 mL) ether. Then the combined organic phase was washed with 30 mL wateter (3 × 10 mL). The ether was dried with $MgSO_4$ at room temperature overnight. The solvent was dried under reduced pressure and the crude product was isolated as brownish solid (9 g). The solid was refluxed with *n*-hexane for 3 h and heat-filtered after treated with activated carbon for 20 min. Then, *n*-hexane was distilled to obtain a deep-yellow acicular crystal (48%). ^{1}H-NMR ($CDCl_3$): δ = 7.95 (Ph—H, 2H, m), 8.24 (Ph—H, 2H, m), 9.43 (N=CH, 1H, s), 10.29 (CHO, 1H, s); ^{13}C-NMR($CDCl_3$):δ = 129.6, 130.4, 131.1, 132.8, 141.9, 142.4, 144.5, 146.0, 192.7; Mp = 106.6–107.2 °C.

2.3.3. Synthesis of 1,4-bisdesoxycyadox

2-Formoxyl-quinoxaline (2 g) was dissolved with 95% ethanol (25 ml). Neohydrazid (1.2 g) in 5 ml water was added to a 100 ml round-bottom flask and stirred for 3 h. The solution was crystallized under −4 °C and filtered. A white solid was obtained, with a yield of 3 g (95%). The whole synthesised path is illustrated in Fig. 1.

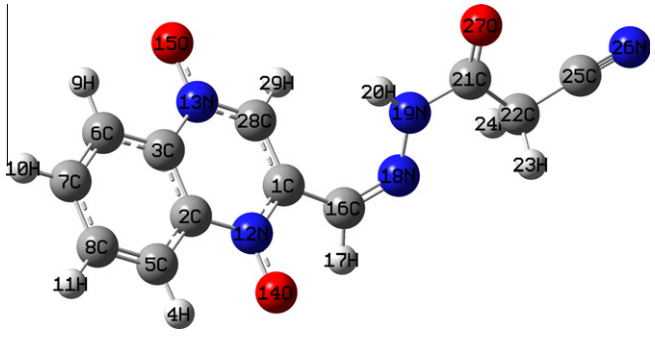

Fig. 2. Optimized molecular structures and atomic numbering of cyadox.

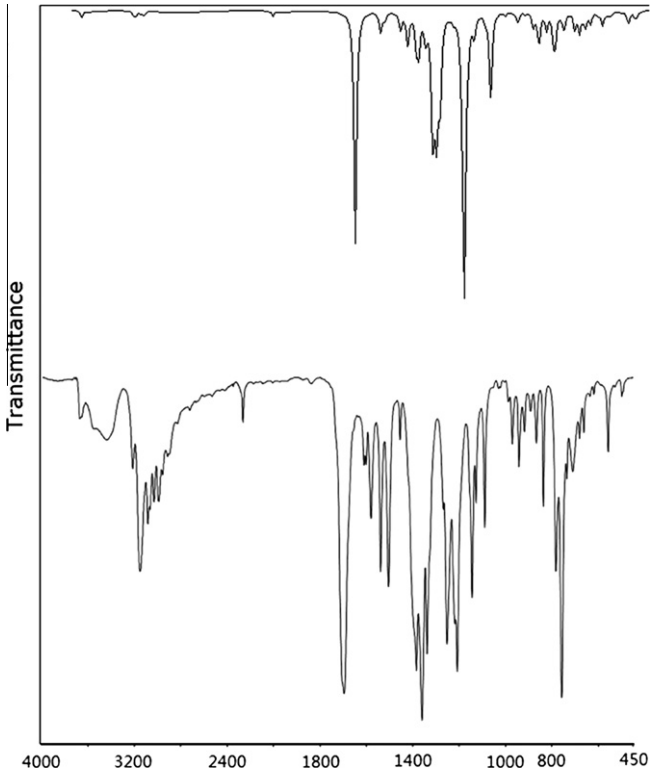

Fig. 3. Calculated FT-IR (upside) and experimental (downside) spectrums of cyadox.

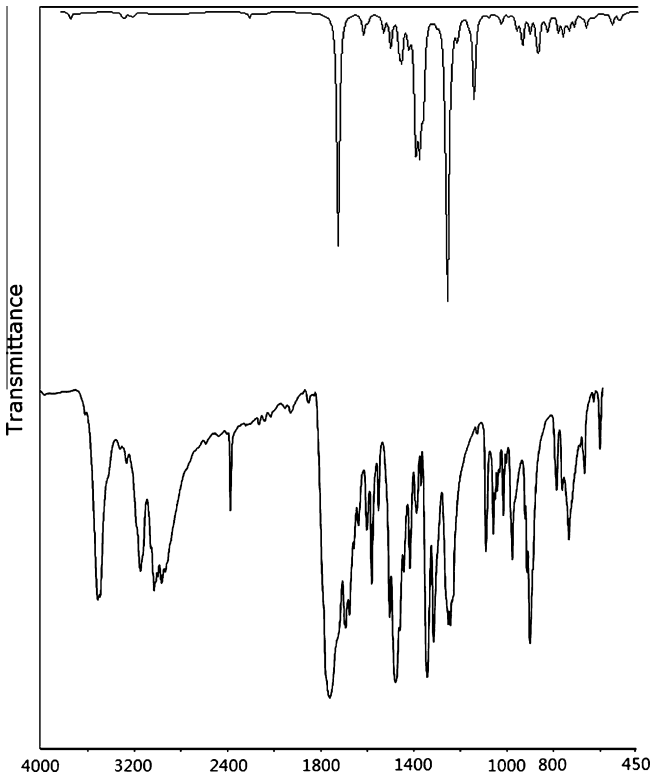

Fig. 4. Calculated FT-IR (upside) and experimental (downside) spectrums of 1,4-bisdesoxymequindox.

Table 2
The observed FT-IR, calculated frequencies using B3LYP/6-31G(d,p) and scaled data with their relative intensities.

Cyadox					1,4-BDC				
Unscaled	Scaled	Intensity	Observed	Proposed assignments	Unscaled	Scaled	Intensity	Observed	Proposed assignments
644.41	651.9496	651.9496			631.59	638.9796	29.341	633.9	ωN17—H18
659.23	666.943	666.943		τC—C(ring)	692.63	700.7338	19.6106		
675.95	683.8586	683.8586			701.23	709.4344	2.8346		
699.61	707.7954	707.7954			781.71	790.856	17.601		
752.45	761.2537	761.2537	757.38	δC—C(ring)	785.07	794.2553	75.4873	792.9	ωC—H(ring)
769.09	778.0884	778.0884			813.11	822.6234	24.0455		
795.65	804.9591	804.9591		ωC—H(ring)	829.56	839.2659	6.3874		
805.64	815.066	815.066			853.24	863.2229	128.7664	859.21	νC19—C20
839.67	849.4941	849.4941			898.62	909.1339	9.7762	899.65	
875.8	886.0469	886.0469	866.35	νsC21—C22	905.2	915.7908	0.877		
886.38	896.7506	896.7506	891.6	δC16—H,δC28—H(ring)	922.81	933.6069	13.9699	926.68	ωC14—H15
902.59	913.1503	913.1503		δC16—H,δC—H(ring)	947.81	958.8994	3.3562	945.31	ρCH2
906.11	916.7115	916.7115	917.85	δC16—H,δC—H(ring)	967.78	979.103	9.1105		
948	959.0916	959.0916	941.65	ρCH_2	990.02	1001.603	1.1405		νC20—C23
981.61	993.0948	993.0948			990.92	1002.514	9.6866		νC20-C23
991.51	1003.111	1003.111		νsC22—C25	998.35	1010.031	2.846	978.19	δsC—H(ring)
1006.9	1018.681	1018.681		τ(ring)	1022.92	1034.888	0.0025	1016.88	δsC—H(ring)
1029.2	1041.242	1041.242		τ(ring)	1031.22	1043.285	4.3696		νC7—C8(ring)
1042.71	1054.91	1054.91	1088.79	δs(ring)	1110.98	1123.978	158.3673		νsN16—N17
1115.34	1128.389	1128.389			1151.05	1164.517	6.9885	1148.57	ρC—H(ring)
1118.3	1131.384	1131.384	1126.98	νsN—N	1163.07	1176.678	2.5063		ρC—H(ring)
1141.94	1155.301	1155.301			1224.17	1238.493	0.0779	1214.57	τCH2
1189.82	1203.741	1203.741			1236.74	1251.21	4.8385		
1199.63	1213.666	1213.666			1242.51	1257.047	29.6208	1243.79	
1225.86	1240.203	1240.203		τCH_2	1253.45	1268.115	357.8089		ωCH2
1227.48	1241.842	1241.842			1305.23	1320.501	0.216	1291.98	δsC—N(ring)
1247.23	1261.823	1261.823			1315.26	1330.649	0.7127	1320.69	νC—N(ring),νC—C(ring)
1257.9	1272.617	1272.617			1346.51	1362.264	4.5508	1349.55	
1300.3	1315.514	1315.514			1374.39	1390.47	221.8208		
1367.39	1383.388	1383.388			1388.86	1405.11	36.6757	1386.95	νC—C(ring)
1376.36	1392.463	1392.463	1359.17	vring,δsCH2,νN12—O14(ring)	1401.51	1417.908	14.1606	1413.03	ρC14—H15
1386.32	1402.54	1402.54	1384.01	vring,δsCH2	1434.7	1451.486	19.6322		δsCH2
1398.88	1415.247	1415.247		vring,δsCH2,νN13—O15(ring)	1452.28	1469.272	8.8134		ω(ring)
1406.37	1422.825	1422.825			1468.52	1485.702	114.8119	1463.61	ωN17—H18
1435.28	1452.073	1452.073	1454.15	δsCH_2	1503.57	1521.162	21.127	1494.23	νs(ring)
1443.02	1459.903	1459.903			1527.75	1545.625	28.0718	1515.94	νs(ring)
1474.03	1491.276	1491.276			1577.34	1595.795	8.68	1574.2	νs(ring)
1486.58	1503.973	1503.973	1503.94	vring	1597.55	1616.241	2.0552	1594.27	νs(ring)
1529.15	1547.041	1547.041	1537.92	vring	1650.23	1669.538	7.8883	1611.2	νas(ring)
1564.25	1582.552	1582.552	1579.22	vring	1666.97	1686.474	39.8599		νsC14—N16
1639.74	1658.925	1658.925		vring	1784.64	1805.52	450.9498	1778.51	νsC19—O25,ωCH2,ωN17—H18
1642.94	1662.162	1662.162		vring	2370.03	2397.759	11.507	2264.33	νsC23—N24
1663.75	1683.216	1683.216			3064.25	3100.102	3.1966	2954.09	νsC20—H
1789.48	1810.417	1810.417		$\nu sCO,\omega CH_2,\omega N—H$	3094.12	3130.321	0.5998	3077.69	νasC20—H
2370.84	2398.579	2398.579	2262	νsCN	3155.13	3192.045	10.005		νsC26—H15
3063.82	3099.667	3099.667	3029.67	νsCH_2	3167.84	3204.904	3.1123		νsC14—H27(ring)
3093.6	3129.795	3129.795	3083.1	$\nu asCH_2$	3179.14	3216.336	1.7506		νasC—H(ring)
3183.79	3221.04	3221.04	3150.55	νsC—H	3190.4	3227.728	3.3602		νsC—H(ring)
3188.84	3226.149	3226.149		νasC—H(ring)	3201.78	3239.241	4.66		νasC—H(ring)
3202.22	3239.686	3239.686		νsC—H(ring)	3206.01	3243.52	10.4197	3203.4	νsC—H(ring)
3230.5	3268.297	3268.297		νasC—H(ring)	3509	3550.055	19.0639	3464.17	νsN17—H18
3232.55	3270.371	3270.371		νsC—H(ring)					
3242.66	3280.599	3280.599	3213.72	νsC—H(ring)					
3496.42	3537.328	3537.328	3440.66	νsN—H					

3. Results and discussion

3.1. Geometrical structure

The initial task for the calculation was to determine the optimized geometries of the title compounds. Due to the unavailability of the exact crystal structures of these compounds, the optimized structures can only be compared with 3-methylquinoxaline-2-carboxilic acid 4-oxide (determined by X-ray studies) [13], which share highly similar quinoxaline structures with cyadox and 1,4-bisdesoxycyadox. The optimized parameters (bond lengths, bond angles) were compared with the experimental data listed in Table 1, in accordance with the atom numbering scheme of cyadox shown in Fig. 2.

As shown in Table 1, some bond lengths are shorter than the experimental values. For example, C2—C5, C3—C6, and C6—C7 experimental bond lengths are 1.404, 1.401, and 1.377, respectively, whereas the calculated bond lengths for cyadox are 1.401, 1.399, and 1.375. This difference is caused by two N—O bonds in the cyadox which exhibit stronger interaction than the experimental compound. Most of the computed bond lengths are slightly larger than the experimental data in the crystal. This result is related to the fact that the experimental data belong to the solid phase, whereas the theoretical calculations are based on the gaseous phase. Therefore, the intermolecular coulombic interactions among neighboring molecules were ignored during calculation. The differences between cyadox and 1,4-bisdesoxycyadox are also notable. Without the strong N—O bond, several calculated bond

Table 3
Computed, scaled and experimental NMR data for cyadox and 1,4-BDC.

Cyadox				1,4-BDC			
	Cal.	Scaled	Exp.		Cal.	Scaled	Exp.
C1	139.17	135.68	137.31	C1	139.49	135.99	142.84
C2	147.31	143.60	137.76	C2	146.65	142.96	143.15
C3	147.50	143.78	138.00	C3	146.88	143.19	147.99
H4	9.04	9.02	9.05	H4	8.98	8.96	9.52
C5	128.04	124.84	119.95	C5	126.67	123.51	129.21
C6	128.32	125.12	120.13	C6	126.58	123.42	130.92
C7	137.97	134.52	132.24	C7	139.30	135.80	131.05
C8	138.24	134.78	132.74	C8	139.34	135.84	130.98
H9	8.99	8.97	8.54	H9	8.91	8.89	8.19
H10	8.08	8.09	8.49	H10	8.30	8.30	8.13
H11	8.08	8.08	8.49	H11	8.29	8.29	8.13
C16	134.56	131.19	133.74	C16	135.61	132.21	141.30
H17	7.76	7.77	7.99	H17	7.82	7.83	7.88
H20	8.92	8.90	7.97	H20	9.22	9.20	7.91
C21	171.55	167.20	165.90	C21	173.06	168.66	165.67
C22	26.96	26.46	24.50	C22	26.77	26.27	24.58
H23	3.86	3.98	4.43	H23	4.16	4.27	2.52
H24	3.78	3.90	4.43	H24	4.12	4.23	2.52
C25	115.70	112.83	116.02	C25	120.82	117.82	116.05
C28	133.69	130.34	127.70	C28	135.58	132.18	129.23
H29	8.55	8.54	12.37	H29	8.68	8.67	12.29
MAE	3.38	2.2		MAE	3.21	2.56	

MAE: mean absolute error.

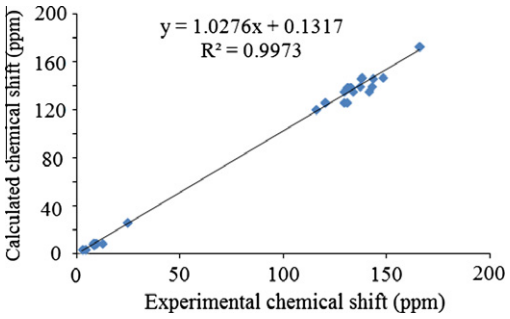

Fig. 5. The linear regression between the experimental and theoretical ^{1}H and ^{13}C NMR chemical shifts of title compounds.

lengths, namely, C2—N12, C1—N12, C3—N13, and N13—C28, are shorter than their parental compounds. In cyadox and 1,4-bisdesoxycyadox, the theoretical results of the C—C—C angles for the benzene ring fall on the typical hexagonal angle of 120°. This finding is in contrast to the quinoxaline moiety, in which substitution leads to some changes in the bond angles. This finding is consistent with the characteristics of other substituted quinoxalines[14].

3.2. Vibrational frequency

DFT revolutionalized theoretical modeling. The development of exchange-correlation functions made possible the calculation of several molecular properties with good performance. DFT calculations on harmonic frequencies provide better vibrational frequencies for organic compounds when proper scaling factor is chosen to correct the calculated frequencies, thus compensating for the approximate treatment of electron correlation, unharmonious effects, and basis set deficiencies [15]. Therefore, in this study, theoretical harmonic frequencies were scaled by the factor for B3LYP/6-311+G(d,p) to correct the theoretical error [16]. IR spectrums from the experiment and B3LYP method are shown in Fig. 3 and Fig. 4. Assignment of several vibrational frequencies in both theoretical and experimental FT-IR are listed in Table 2.

The characteristic C—H stretching vibrations in the quinoxaline heteroaromatic ring were observed above 3000 cm^{-1}. In the experimental spectrum, the C—H stretching frequencies were 3213.7 cm^{-1} for cyadox and 3203.4 cm^{-1} for 1,4-BDC. The theoretical vibrations assigned to the same type of vibration were 3268.3, 3270.4, and 3280.6 cm^{-1} for cyadox and 3227.7, 3239.2, and 3243.5 cm^{-1} for 1,4-BDQ. The intense deformation band and the scissoring C—H bond of the methyl and methylene groups lie in 1386.0–1454.2 cm^{-1} for cyadox and 1268.1–1451.5 cm^{-1} for 1,4-BDC. The C—H vibrations of in-plane were observed at 917.9 and 945.3 cm^{-1} for the title compounds.

Majority of the C—C and C—N vibrations are bound to the whole ring, so these frequencies are discussed together with the skeletal vibrations. Wave numbers occurring within 1503.9–1662.2 cm^{-1} for cyadox and 1494.2–1686.5 cm^{-1} for 1,4-BDC were assigned to the ν C—C (ring) and the ν C—N (ring). These specific bands were found in the experiment IR spectrum of our previous quinoxaline molecule study [17]. Cyadox shows a strong band at 1359.2 cm^{-1}, assigned to the stretching N=O in the experimental spectrum. The calculated value is predicted to be 17 cm^{-1} higher at 1376 cm^{-1}. These vibrational frequencies cannot be seen for 1,4-BDC.

3.3. NMR spectra

The characterization of the compound was further enhanced by the use of ^{1}H and ^{13}C NMR spectroscopy. The ^{1}H and ^{13}C NMR spectra of the title compounds were recorded using TMS as an internal standard and dimethylsulfoxide (DMSO-d_6) as solvent. GIAO ^{1}H and ^{13}C chemical shift values (with respect to TMS) were calculated using the B3LYP method with the 6-311G(d,p) basis set and compared with the experimental ^{1}H and ^{13}C chemical shift values. The calculated ^{1}H and ^{13}C isotropic chemical shieldings for TMS at the B3LYP/6-311++G(2df,2dp) level in DMSO through the IEFPCM method were 31.71 and 184.55 ppm. The theoretical and experimental chemical shifts, isotropic shielding tensors, and peak assignments for cyadox and 1,4-BDC are summarized in Table 3.

The linear correlation between the calculated and experimental values was determined, and the results are presented in Fig. 5. A good correlation between predicted and observed 13C and 1H chemical shifts was found. Moreover, the slope and intercept of the least-square correlation lines were used to scale the GIAO isotropic absolute shielding constants r and to scale chemical shifts in

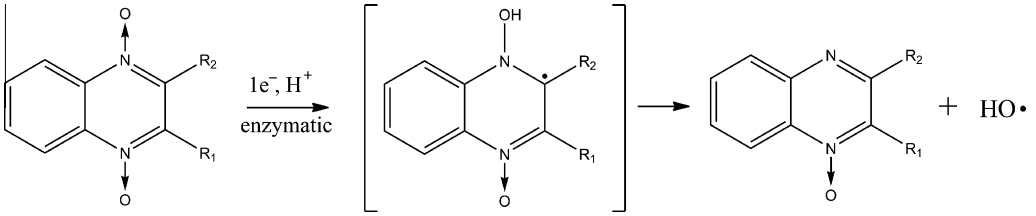

Fig. 6. Enzimatic reduction of QdNO derivatives drug yielding radical intermediates.

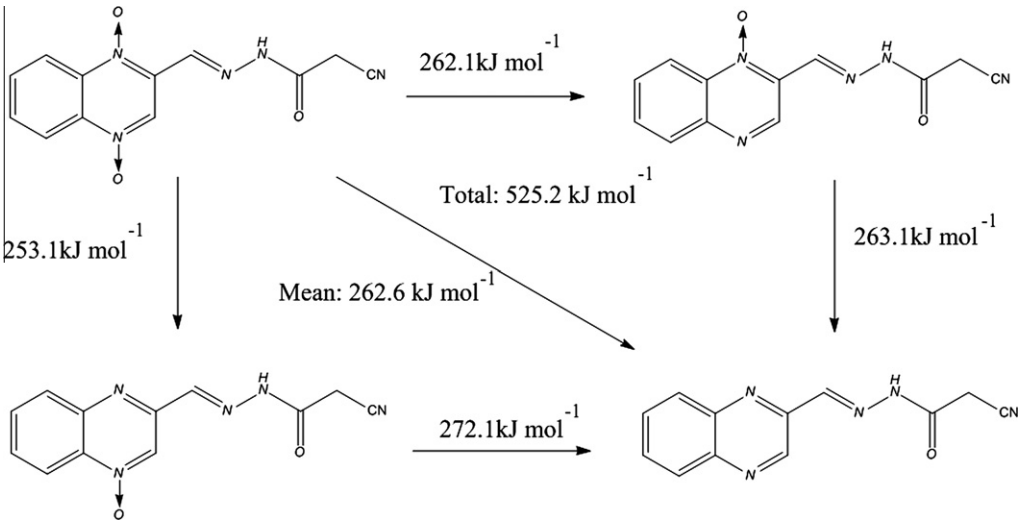

Fig. 7. First, second, total and mean N—O BDEs for cyadox were computed at the B3LYP/6-311++G(2df,2dp) level of theory.

the equation $\delta = (\delta_{calc}\text{-intercept})/\text{slope}$. In this study, the intercept and slope for B3LYP/6-311++G(2df,2dp) level combined with IEFPCM solvent model are −0.2271 and 1.0274, respectively. Results of the comparison with experimental observations are presented in the correlation graphs based on the calculations. The correlation coefficient is 0.9967. As shown in Table 3, the mean absolute values for cyadox and 1,4-BDC are 3.38 and 3.21, whereas the corrected MAE is 2.2 and 2.56 ppm.

The chemical shifts of carbon atoms belonging to the quinoxaline moiety observed over 120 ppm are obviously higher than the carbon on the branched chain C22 and C25, except for C21. This phenomenon is due to the carbonyl (C=O) atom. The differences of chemical shifts between cyadox and 1,4-bisdesoxycyadox are also obvious. In this study, the ^{13}C chemical shifts of quaternary carbons C2, C3, C1, and C28 of 1,4-BDC are higher than those of cyadox in terms of the differences in the electronic interactions with the O atom. Moreover, with the metabolizing of O atom which belongs to the N—O bond, the inductivities of the N atom to H atom decrease. The loss of O atom also increases the electron density on the whole conjugate ring. Based on these observation, the chemical shifts of H9, H10, H11, and H29 are high and experimentally observed as 8.19, 8.13, 8.13, and 12.29 in 1,4-BDC.

3.4. N—O BDE calculation

With the development of QdNO derivatives and progress in drug safety, several studies which feature experimental validation or theoretical calculation resulted in remarkable achievements. The most important highlights of these breakthroughs are the radical intermediates that they enzymatically reduced in vivo, causing cytotoxic DNA strand breaks and pharmaceutical effect. This mechanism (Fig. 6) is widely accepted by the formation of these intermediates including drug radical and hydroxyl radical, which is directly dependent on the N—O bond [18]. Therefore, the measure and evaluation of N—O bond strength is important for systematic research of QdNOs drugs. For example, the high N—O BDE of tirapazamine (TPZ) yields corresponding activated TPZ, which causes high DNA damage. However, limited N—O BDE data are available for QdNO veterinary drug. However, studying this structure-related parameter for cyadox is necessary. In this study, the first, second, total, and mean N—O BDE of cyadox are calculated in B3LYP/6-311++G(2df,2dp) level of theory. Typically, the first N—O BDE is the energy required to break the weaker bond in the di-N-oxide compound to yield the corresponding N-oxide, whereas the second N—O BDE is the energy required to break the other bond. The total and mean N—O BDE are the sum and mean of the dissociation enthalpies that form the corresponding N-oxide.

The calculated values for the BDE of cyadox are schematically depicted in Fig. 7. The dissociation of the 12N—14O bond, which is closer to the branched chain, occurred easily than the 13N—15O bond and yielded a first BDE value of 253.1 kJ mol^{-1}. The energy required to remove the 15O atom was 262.1 kJ mol^{-1}, almost 10 kJ mol^{-1} higher than the first O atom. The corresponding value of the total and mean N—O BDE were 525.2 and 525.2 kJ mol^{-1}, respectively.

4. Conclusion

In this study, 1,4-Bisdesoxycyadox, a main deoxidized metabolite of cyadox, was synthesised and characterized by spectroscopic techniques (FT-IR and NMR). To support the solid-state structure, geometric parameters were optimized using B3LYP method with 6-311+G(d,p) basis set. The results were compared with the X-ray diffraction data of similar molecular compounds. From the optimized geometry of the molecule, vibrational frequencies of the title compounds were calculated via B3LYP/6-311+G(d,p) approach and compared with the experimental data. The magnetic isotropic shielding constants were calculated using GIAO/B3LYP/6-311++G(2df,2pd) method. Linear correlations with the experimental ^{1}H and ^{13}C chemical shifts were obtained. The computed chemical shifts, scaled by the linear correlation equation, produced the experimental results with MAE lower than 2.2 ppm. Moreover, the first, second, total, and mean N—O bond dissociation enthalpies (BDEs) were obtained theoretically. The predicted values based on 6-311++G(2df,2pd) were 253.1, 262.1, 525.2, and 525.2 kJ mol^{-1}, respectively.

Acknowledgements

This work was supported by 973 Fund, the Ministry of Science and Technology, P.R. China (Grant No. 2009CB118801), the National Natural Science Foundation of China (Project No. 20977112), Program for New Century Excellent Talents in University and the Specialized Research Fund for the Doctoral Program of Higher Education of China New Teachers' Fund for Doctor Stations, Ministry of Education (Grant No. 20090008120015).

References

[1] D. Zhao, L. He, C. Pu, A. Deng, Anal. Bioanal. Chem. 391 (2008) 2653.
[2] Q. Chen, S. Tang, X. Jin, J. Zou, K. Chen, T. Zhang, X. Xiao, Food Chem. Toxicol. 47 (2009) 328.
[3] X. Wang, Q. He, Y. Wang, A. Ihsan, L. Huang, W. Zhou, S. Su, Zhen Liu, Z. Yuan, Regul. Toxicol. Pharm. 59 (2011) 324.
[4] X. Huang, H. Zhang, X. Wang, L. Huang, L. Zhang, C. Yan, Y. Liu, Z. Yuan, Chem-Biol. Interact. 185 (2010) 227.
[5] H.C. Zhang, C. Huang, Environ. Sci. Technol. 39 (2005) 593.
[6] L. Huang, Y. Wang, Y. Tao, D. Chen, Z. Yuan, J. Chromatogr. B 874 (2008) 7.
[7] Z. Liu, L. Huang, M. Dai, D. Chen, Y. Wang, Y. Tao, Z. Yuan, Rapid Commun. Mass Spectrom. 22 (2008) 1009.
[8] P.J. Stephens, F.J. Devlin, C.F. Chabalowski, M.J. Frisch, J. Phys. Chem. 98 (1994) 11623.
[9] A.D. Becke, J. Chem. Phys. 98 (1993) 5648.
[10] C. Lee, W. Yang, R.G. Parr, Phys. Rev. B 37 (1988) 785.
[11] E. Cancès, B. Mennucci, J. Tomasi, J. Chem. Phys. 107 (1997) 3032.
[12] M.J. Frisch, G.W. Trucks, H.B. Schlegel, G.E. Scuseria, M.A. Robb, J.R. Cheeseman, G. Scalmani, V. Barone, B. Mennucci, G.A. Petersson, H. Nakatsuji, M. Caricato, X. Li, H.P. Hratchian, A.F. Izmaylov, J. Bloino, G. Zheng, J.L. Sonnenberg, M. Hada, M. Ehara, K. Toyota, R. Fukuda, J. Hasegawa, M. Ishida, T. Nakajima, Y. Honda, O. Kitao, H. Nakai, T. Vreven, J.A. Montgomery, J.E. Peralta, F. Ogliaro, M. Bearpark, J.J. Heyd, E. Brothers, K.N. Kudin, V.N. Staroverov, R. Kobayashi, J. Normand, K. Raghavachari, A. Rendell, J.C. Burant, S.S. Iyengar, J. Tomasi, Gaussian 09, ReVision A.02, Gaussian, Inc., Wallingford, CT, 2009.
[13] Y.B. Li, W.F. Zhou, J.L. Wang, H.X. Gao, Z.Q. Zhou, Acta Cryst. E 66 (2010) o1801.
[14] Ş. Yurdakul, T. Polat, J. Mol. Struct. 963 (2010) 194.
[15] E. İnkaya, M. Dinçer, Ő. Ekici, A. Cukurovali, J. Mol. Struct. 1026 (2012) 117.
[16] J.P. Merrick, D. Moran, L. Radom, J. Phys. Chem. A 111 (2007) 11683.
[17] J.H. Zhang, X. He, H.X. Gao, J. Mol. Struct. 1004 (2011) 109.
[18] J.R.B. Gomes, M.D.M.C. Ribeiro da Silva, M.A.V. Ribeiro da Silva, Chem. Phys. Lett. 429 (2006) 18–22.